IEEE Access
Multidisciplinary | Rapid Review | Open Access Journal

Received May 27, 2019, accepted June 6, 2019, date of publication June 14, 2019, date of current version June 28, 2019.

Digital Object Identifier 10.1109/ACCESS.2019.2923073

Microwave Induced Electroporation of Adherent Mammalian Cells at 18 GHz

SÖNKE SCHMIDT[1], (Student Member, IEEE), MARTIN SCHÜßLER[1], CAROLIN HESSINGER[1], CHRISTIAN SCHUSTER[1], (Student Member, IEEE), BIANCA BERTULAT[2], MARINA KITHIL[3], M. CRISTINA CARDOSO[3], AND ROLF JAKOBY[1], (Member, IEEE)

[1]Institute of Microwave Engineering and Photonics, Technische Universität Darmstadt, 64283 Darmstadt, Germany
[2]Department of Biochemistry, Chemistry and Pharmacy, Johann Wolfgang Goethe University Frankfurt, 60323 Frankfurt, Germany
[3]Institute of Cell Biology and Epigenetics, Technische Universität Darmstadt, 64283 Darmstadt, Germany

Corresponding author: Sönke Schmidt (schmidt@imp.tu-darmstadt.de)

This work was supported by the Technische Universität Darmstadt through the Forum for Interdisciplinary Research and the Activator Fund.

ABSTRACT This paper discusses microwave-induced electroporation as a promising alternative to conventional transfection methods. Adherent C2C12 mouse cells are successfully transfected with a 5TAMRA red-labeled peptide by using a recently developed planar microwave electroporation tool. It allows to monitor the uptake kinetics with live-cell confocal microscopy and is suitable to culture, manipulate, and observe the adherent cells over several days. Viability tests with the Calcein blue AM proof the vitality of the treated cells after 72 h. The question of whether the observed effects are temperature or field induced is tackled. For this reason, comprehensive coupled full-wave electromagnetic-thermal simulations are aligned with temperature measurements. The temperature at the position of the cells does not exceed 34 °C for an input power of 24 dBm. The corresponding electric field strength is evaluated at the position of the cells. A value of 150 V/cm is not exceeded, which is at least a factor of 10 below the field strength of the conventional electroporation. Consequently, almost no cell mortality does occur during the treatment. Comparative thermal tests without a microwave field but with a successively increased temperature up to 42 °C show no uptake. In contrast, the successful uptake follows the pattern of the microwave field although the temperature distribution is homogeneous. We rate this as evidence that the uptake is induced by the high-frequency electromagnetic field rather than the temperature.

INDEX TERMS Electroporation, exposure system, cells, transfection.

I. INTRODUCTION

One of the most challenging steps for any therapeutic drug to work is to cross the barrier of the cell's plasma membrane to reach their molecular targets, in order to interact with a specific intracellular protein to disrupt or activate a given cellular circuit. Cells are individualized by phospholipid bilayers effectively separating the cell's interior from the extracellular environment. This essential barrier function causes a hurdle for the delivery of a variety of compounds such as drugs, DNA, RNA or peptides into the cell. Consequently, studying and manipulating intracellular metabolism is limited by the methods available for intracellular delivery of molecules. Although different physical (micro-injection, electroporation), chemical (cationic lipids and polymers) and biological (virus infection) methods have been developed, their efficacy and applicability strongly varies and is in need of continuous optimization. Electroporation is the most versatile method of the before mentioned as it is not limited to a specific substance to be delivered or by the type of cells to be used. Since 1982 it is known that the membrane can be overcome by exogenous molecules by applying an electric field for a certain time [1]. Albeit generally applicable to different cell types, electroporation commonly requires cells to be in suspension, i.e., cells growing on a substrate need to be first detached usually by an enzymatic digestion step, electroporated and subsequently seeded on the substrate to re-attach. This protocol involves several steps and time, greatly reduces cell viability as a large portion of the cells die during the procedure and does not allow continuous monitoring of the effects before, during and after the delivery of the substance by electroporation. In fact, most often, the reattachment of the cells alone requires several hours and the observation of the effects can only be started the

The associate editor coordinating the review of this manuscript and approving it for publication was Haiwen Liu.

next day. The low viability of the cells upon electroporation intrinsically limits this method to cells available in large amounts (e.g., tumor cells). Usually pulsed electric fields are used [2], [3] but successful continuous wave (cw) electroporation is also documented [4], [5], [6]. Moreover, high magnetic field pulses (5.5 T) with low electric field strengths [7], [8] were used as an alternative to conventional electroporation or in combination [9].

The necessary field strength as well as the pulse length and frequency highly depends on the application and the type of cell but are still ongoing topics in current research. Mechanisms were investigated and simulated on molecular level in depth [10], [11], but still not fully understood [12]. The applied pulses can be in the range of milliseconds down to nanoseconds while the electric field strength is in the range of 1 to 20 kV/cm. Current research even focus on sub-nanosecond pulses and its ability to target intracellular structures, which was summarized in great detail in [13].

In general the electric field applied leads, depending on its direction relative to the cell, to an increased or decreased transmembrane potential (hyperpolarization or depolarization). This causes pore formation as well as an increased conductivity of the cell membrane. The minimal required external electrical field strength is related to the transmembrane potential of the cell, its radius as well as the required size of the pores. Higher field strengths increase the uptake efficiency with the drawback of reducing the cell viability. In contrast to conventional electroporation recently, successful electroporation with significantly lower field strength at microwave frequencies (18 GHz) was reported [14], [15], [16]. In [14], cw signals instead of pulses were used to transfect Gram-positive cocci. An experimentally determined specific absorption rate (SAR) of 5 kW/kg was reported. With an efficiency of 97 % pores of at least 23.5 nm were measured, with a pore lifetime of 9 min. In [16] *Escherichia coli* bacteria were permeabilized with a field strength of only 300 V/m at 18 GHz below a critical temperature of 40 °C. Uptake of 150 kDa fluorescein isothiocyanate was reported with a cell recovery rate of 88 %. A temporary morphological change was monitored after microwave treatment in comparison to a control test under the same thermal conditions. In [15] permeabilization of red blood cells (which are cultured in suspension) with a cell viability of up to 94% was shown at 18 GHz. All above mentioned publications have in common that they use continuous wave microwave fields at 18 GHz, with a dramatically reduced field strength ($\approx$ 300 V/m) and high viability rates. Because the resulting potential differences at the cell membrane are lower than the reported minimal values, it was suggested that the uptake mechanism differs. Due to the high losses induced by the resonance of water in this frequency region ($\tan\delta \approx 0.88$ at 20 °C, $\tan\delta \approx 0.63$ at 35 °C for $f = 18$ GHz, [17]) it is likely that this effect is linked to an electrokinetic modification at the cell surface. While the addition of sodium chloride in the buffer medium changes the resonance frequency slightly its influence is negligible for practical mixtures [18].

Devices for electroporation range from simple parallel plate capacitors in cuvette to impedance matched broadband designs for sub-nanosecond pulses [19]. The use of microwave frequencies require advanced applicators to deliver the field strength to the cells. The system used in [16] is based on a closed microwave resonator. As the uptake mechanism seems to differ from conventional electroporation, it is beneficial to monitor the uptake process optically. In addition, optical monitoring is non-invasive, thus, enabling real time observation. Therefore, in [20] we demonstrated an approach for exploring the field of microwave assisted electroporation. While the general proof of concept was shown with the permeabilization of SF9 insect cells that were cultured in suspension, poor optical resolution did not allow a continuous monitoring of the process. The viability was only assessed on the basis of the cells morphology. Moreover, exact estimations of the electrical field strength and the temperature at the spot of the cells were not made.

In this paper, the delivery of fluorescent-labeled peptides (Pep-5T) into adherent C2C12 mouse muscle cells with microwave fields at 18 GHz is demonstrated. As mentioned above, usually, electroporation requires bringing adherent cells into suspension for the treatment and subsequently let them re-adhere onto a substrate before further investigation. To avoid these additional time consuming and cell-stress inducing steps of the protocol, a novel planar applicator was developed which allows for microwave exposure of the cells directly in their native state. The design of the applicator is described in section II. The minimal size of the applicator reduces the amount of potentially costly substances and makes it applicable for limited cell material (e.g., primary patient cells). The process was monitored with confocal microscopy throughout the treatment. After 72 h, viability tests were conducted using the Calcein blue AM staining assay as described in section III. Finally, a comprehensive thermal analysis within the applicator and a field strength estimation is discussed in section IV to tackle the question whether the observed effects are temperature or field induced.

II. APPLICATOR DESIGN

In order to provide high field strength in a lossy medium at microwave frequencies with a limited input power the transducer, loaded with water has to be well matched. Apart from this, for the design of the applicator, several aspects have to be considered: (1) accessibility for microscopic observation, (2) potential cell toxicity of cavity materials, substrate, electrodes as well as the connection between cavity block and substrate, (3) electrode and connection layout, (4) cavity dimensions in relation to cell culture volume and final substance concentration considerations, (5) general dimensions and standard microscope hardware and working dimensions (e.g. stage adapters, objective working distances), (6) general consideration on application of cells, liquids and handling.

An ungrounded coplanar waveguide (cpw) was fabricated on 200 µm thin Schott Mempax^{TM}glass with a relative permittivity of $\varepsilon_r' = 4.7$ and $\tan(\delta) \approx 10^{-2}$. This provides

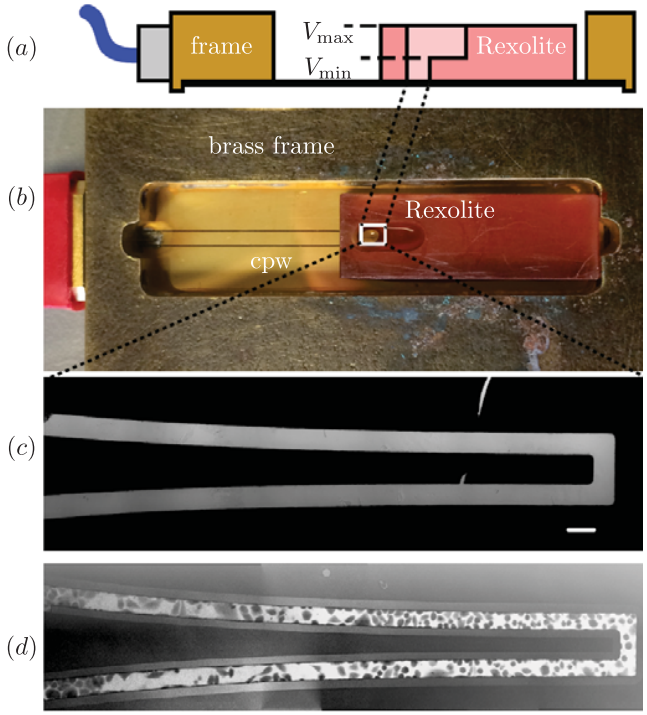

FIGURE 1. Microwave electroporation tool: A cavity with the maximal volume of 90μl allows microwave treatment of mouse C2C12 adherent cells. (a): Cross section of the structure. (b): The thin and fragile glass substrate is mounted with conducting silver glue in a metallic frame. It adds stability, serves as ground for the waveguide and fits to the stage adapter of the microscope. (c) At the bottom of the chamber, the 50μm gap enables live cell microscopy while exposing the cells to a microwave field. (d) shows the cells during the treatment. Scale bar: 50μm.

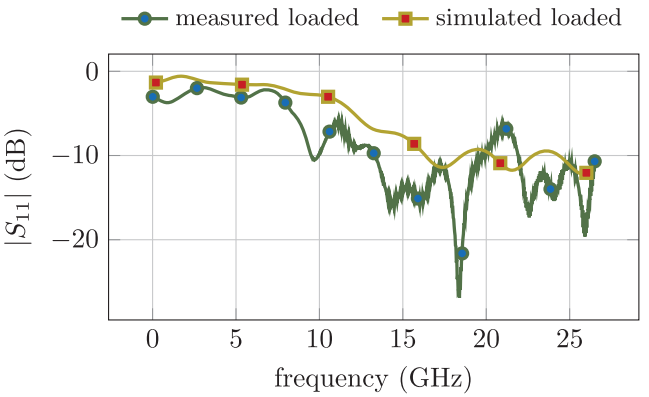

FIGURE 2. The reflection $|S_{11}|$ of the structure was minimized at 18 GHz for the case of a filled reservoir. The simulation of the loaded transducer shows the interaction of the microwave field and the water since $|S_{11}|$ follows the losses of the water. The measurements differ due to standing waves and losses introduced in the realized applicator. However, the fixture is well matched ($S_{11} \leq -10$ dB) around 18GHz.

the possibility and resolution to monitor the uptake process kinetics with live cell confocal microscopy throughout the treatment and observe adherent cells over several days. A gold metalization, which is not harmful for living cells, with a height of $t = 2.5$ µm was plated. The gap size of the coplanar waveguide corresponds to the maximum achievable electric field strength for a given limited input power. For reasons of practical realization the gap was chosen to 50 µm. Moreover, this gap size is suitable to observe all relevant cell sizes i.e. at least one cell is fully visible between the electrodes. On top of the cpw a 90 µL reservoir made out of Rexolite^{TM}was glued. To provide mechanical stability for the thin glass substrate, the applicator was mounted with conducting silver glue in a metallic frame which fits to a common microscope stage adapter as depicted in Figure 1 (a). The frame also serves as the ground of the cpw.

The cpw, as depicted in Figure 1 (b), was tapered in an optimization process with CST microwave studio. In order to provide maximum field strength at the transducer, the reflection at the edge of the container needs to be minimal. Because the open ended transmission line in the container is loaded with a highly lossy material (similar to water) it is possible to match the structure.

Figure 2 depicts the simulated and measured S-parameters of the applicator loaded with cells and water (Figure 1 (c)). The simulation of S_{11} follows the losses of the water. Standing waves and additional losses of the realized applicator (glue, SMA connector, plated gold) introduce differences between the measurement and simulation. However, the measurement still shows the strong interaction of the water in the reservoir and the electric field.

III. EXPERIMENTS AND MEASUREMENTS

Adherent C2C12 mouse cells were incubated with *Pep-5T* with the amino acid sequence LGQQQPFPPQQL-5TAMRA (Biomedal Life Science, Sevilla, Spain) and an estimated molecular weight of MW=1795 g/mol (Pep ca. 1267.39 g/mol; 5T ca. 527.53 g/mol) for 10 to 30 min prior to electroporation process at standard cell culture conditions (i.e. 37 °C, 5 % CO2, humidified atmosphere). All experiments were carried out in PBS and a working concentration of 10 µmol of Pep-5T. After initial incubation, at time t_0, no peptide uptake was visible and cells appeared as dark outlines within the chamber (Figure 1 (d)). Approximately 10 min after microwave field exposure, first effects (blebbing of cell membranes) became visible followed by Pep-5T uptake shortly after. Appearance of positive cells seems to be correlated to microwave field strength starting from the chamber's beginning. Experiments were stopped after $\approx$ 20 min, as the majority of cells within the observation region turned TAMRA-positive (Figure 3 (a)). Afterwards, the electroporation chamber was stored in the incubator. After 72 h Calcein blue AM viability staining was performed (Figure 3 (b)). This revealed viable cells (shown in green) that still contained Pep-5T (shown in red).

IV. ESTIMATION OF ELECTRIC FIELD STRENGTH AND TEMPERATURE

In principle, both temperature and electric field strength are critical parameters for the success of electroporation. They are inherently coupled, since the losses of water (which is

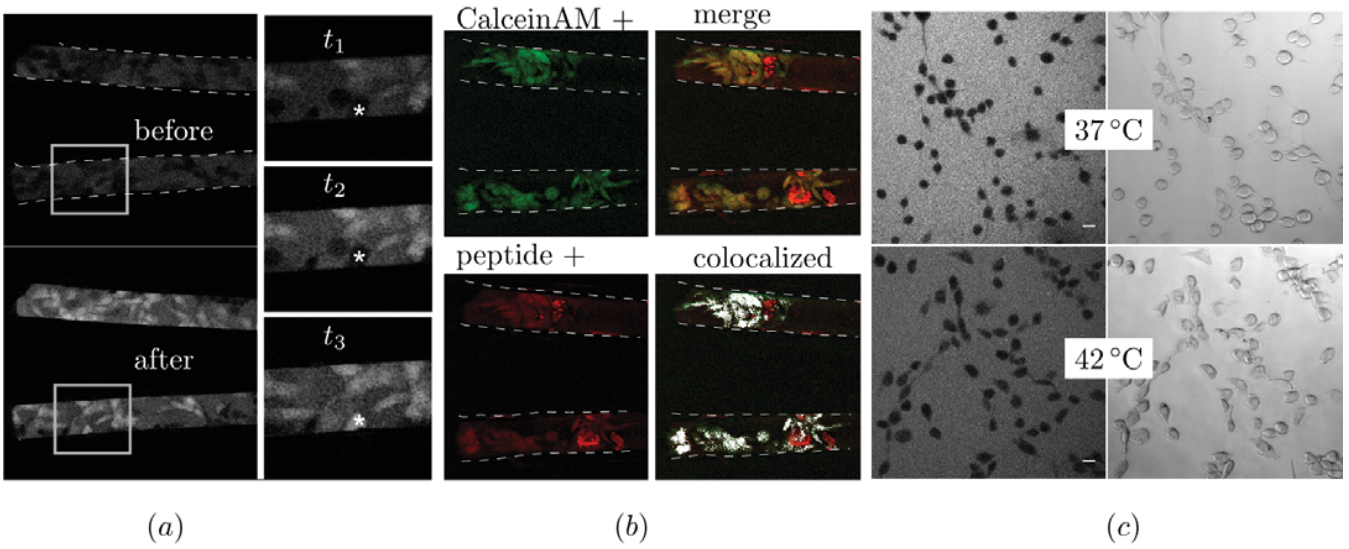

FIGURE 3. Uptake of Pep-5T into adherent cells: Cells were incubated for ca. 10 to 30 min with Pep-5T before microwave exposure (t_0). Time lapse microscopy of peptide uptake by C2C12 cells is shown during the process. At t_1, t_2, and t_3 the marked cell is depicted just before its uptake started, during the process, and right after the successful transfection (a). Magnification of the marked region is shown for better visualization of the uptake process (asterisk). (b) Three days after microwave electroporation, cells were incubated with Calcein blue AM (Life Technologies GmbH, Darmstadt, Germany) live cell dye (shown in green) to monitor viability. Colocalization of living (green) and peptide positive (red) cells is shown by merging color channels. Double positive areas are depicted by white pixels. For better visibility the cpw borders are marked by dashed lines. (c) Control tests with different thermal conditions show no uptake of the peptide. The left side depicts the fluorescent channel, the right side the transmission light. Scale bar: 20μm.

at high frequencies electrically almost identical to the used phosphate buffered saline solution) are high ($\tan(\delta) \approx 1$) at microwave frequencies. Therefore, by increasing the electric field strength, the temperature in the buffer medium and cells also increases. While on the one hand heating can be mortal for cells, on the other hand it is not reported that temperature alone can induce transfection of peptides. However, it is an open question if a certain temperature can influence the uptake efficiency, reduce the necessary time or is even required for successful microwave assisted electroporation of mammalian cells at all. For example, in [21] a thermal pretreatment of the skin to 43 °C led to an enhanced gene transfer induced by electroporation afterwards, which might be based on a higher membrane fluidity. Therefore, it is necessary to evaluate the temperature and keep it constant throughout different experiments.

Besides using higher frequencies, the main difference to conventional electroporation in [14], [15], is the lower electric field strength which was reported to be a key factor for enhancing the cell viability accordingly. As a consequence, knowing the exact value of the electric field strength directly at the transducer is important to assess the experiment. While temperature measurements can be performed relatively simple in such a setup, it is difficult to determine the electric field at the position of the cells. For this reason, at first temperature measurements were conducted. Afterwards, a coupled electromagnetic-thermal simulation was made. By taking into account physical boundaries e.g. ambient temperature, convection and the output power of the source, the thermal simulation model was brought in line with the corresponding

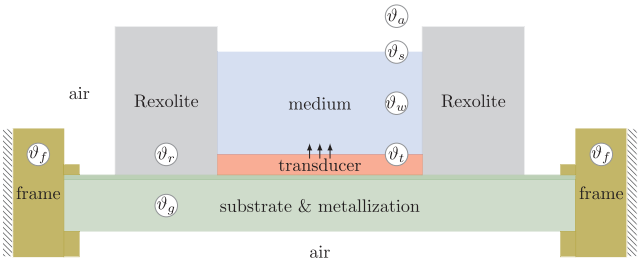

FIGURE 4. The simplified cross section of the applicator shows the structure of the relevant materials for the heat flow. The heat is mainly transferred to the adjacent materials of the transducer i.e. buffer medium, metalization and Rexolite. The different temperatures were measured and matched subsequently to a coupled electromagnetic-thermal simulation.

measurements. Subsequently, the corresponding electric field strength was determined from coupled simulation results.

A. TEMPERATURE

Figure 4 depicts a simplified cross section of the structure to illustrate the heat transport. The heat source is dominated by the dielectric losses of the water. In particular, the 50 µm gap of the transducer is the location where most of the electric field interacts with the aqueous buffer medium, and therefore, the heat spot. Because of the small dimensions, in Figure 4 the transducer in combination with a thin fluid film is assumed to be a homogeneous heat source with a temperature ϑ_t. Because the cells of interest are placed in the gap, ϑ_t is also the maximum temperature they are exposed to. The heat is transferred to surrounding materials, namely

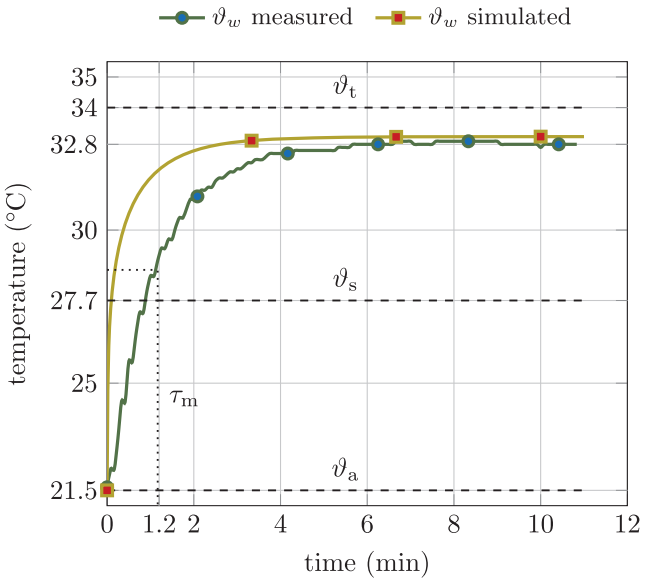

FIGURE 5. Although the volume of the reservoir is low and convection occurs, different temperatures can be measured at the surface, the center and the bottom of the buffer reservoir.

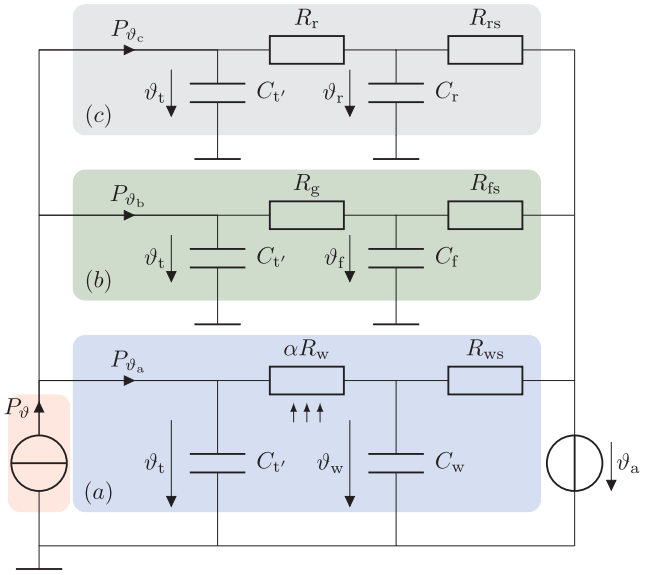

FIGURE 6. The heat flow can be divided in three main parts. The colors of the equivalent thermal circuit matches to colors of the physical arrangement of the structure in Figure 4. Here, (a) is the heat flow through the fluid, (b) represents the path of the substrate combined with the metalization and (c) is the path of the glued Rexolite container. For simplification, cross coupling between the paths was neglected.

the glass substrate ϑ_g, Rexolite container ϑ_r and the fluid in the reservoir with a temperature at the center of the reservoir of ϑ_w. At the surface of the medium an other temperature (ϑ_s) is assumed. Because the metallic frame has a comparatively large surface and good thermal coupling its temperature ϑ_f equals the ambient air temperature ϑ_a.

During the experiment, different temperatures were measured with an input power of $P_\mathrm{i} = 24\,\mathrm{dBm}$ as depicted in Figure 5. The experiments were conducted in a temperature stabilized laboratory with a measured temperature of $\vartheta_a = 21.5\,^\circ\mathrm{C}$. Since the volume of the reservoir is small (90 µL) similar temperatures at the surface, center, and bottom of the reservoirs are expected. This is due to convection, which describes the heat flow caused by temperature induced density differences. Nevertheless, small to medium temperature differences occur. At the surface of the filled reservoir a temperature of $\vartheta_s = 27.7\,^\circ\mathrm{C}$ was measured with an infrared camera. The temperature of the buffer was measured at the center of the reservoir with a fiber optical thermometer (Optocon Fotemp1-4, standard deviation $\pm 0.2\,^\circ\mathrm{C}$, resolution $0.1\,^\circ\mathrm{C}$) which is not affected by the microwave field. The intrinsic time constant of the thermometer was figured out to be smaller than 2 s, and therefore, negligible. However, the time constant of the applicator $\tau_\mathrm{m} = 70\,\mathrm{s}$ can be seen well in the depicted measurement of the water temperature which does not exceed a value of $\vartheta_\mathrm{w} = 32.8\,^\circ\mathrm{C}$. Most important is the temperature, at which the cells are exposed to during the treatment. The temperature sensor of the fiber optic is made out of teflon which has a different dielectric constant than water. Because this difference would eventually affect the field strength and thus, the resulting temperature slightly, a time constant during the heating process at the transducer could not be measured. Instead, the thermometer was dipped several times on the structure after a steady temperature was reached in the buffer medium. A maximum temperature $\vartheta_t = 34\,^\circ\mathrm{C}$ is not exceeded and well below normal culture conditions of the mammalian cells used ($37\,^\circ\mathrm{C}$). Hence, as in control experiments the incubation of cells with TAMRA-peptide at $37\,^\circ\mathrm{C}$ and $42\,^\circ\mathrm{C}$ for up to 1 h does not result in visible peptide uptake (Figure 3 (c)) we conclude that microwave induced heating alone is not sufficient for substance uptake in cells during the time of our microwave experiments.

In order to validate the temperature and determine the electric field strength directly at the transducer, a coupled full wave electromagnetic and thermal simulation of the structure depicted in Figure 1 was performed in CST microwave studio. Figure 6 shows the equivalent circuit of the heat flow which is helpful to determine appropriate physical boundary conditions and assess the simulated temperatures correctly respectively. The heat flow P_ϑ can be divided in 3 parts. The corresponding colors represent the arrangement of the materials in Figure 4. Figure 6 trace (c) corresponds to the heating of the Rexolite container, where $1/R_\mathrm{r}$ and C_r are the thermal conductivity and the thermal capacity of the Rexolite respectively and $1/R_\mathrm{rs}$ is the thermal conductivity to the surface. Trace (b) sums up the heat flow through the substrate (R_g) and the frame (C_f, R_fs), where the letter is assumed to be negligible small and thus, the temperature of the frame ϑ_f equals the ambient temperature ϑ_a. Therefore, the frame was neglected for the simulation and replaced by isothermal boundary conditions. Both traces, (b) and (c) are comparatively well represented in the simulation since all thermal properties, apart from the glue of the container as

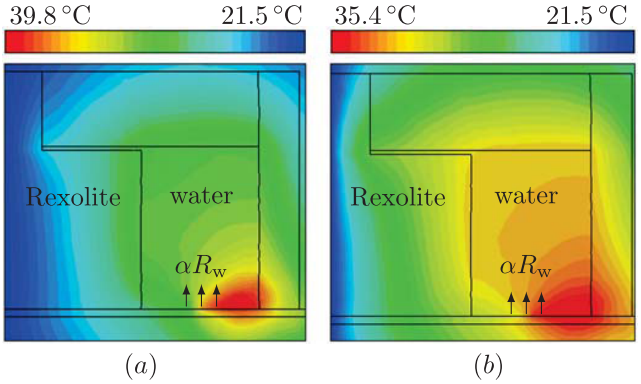

FIGURE 7. Simulated temperature distribution inside the reservoir filled with water. The heat is caused by the interaction of water and electric field. Different values of the thermal conductivity coefficient α results in both, differences in temperature distribution and maximum temperature. While (a) depicts the temperature without convection ($\alpha = 1$), (b) shows a simulation with $\alpha = 1/2$ which mimics convection and results in similar temperature distributions as the measurements.

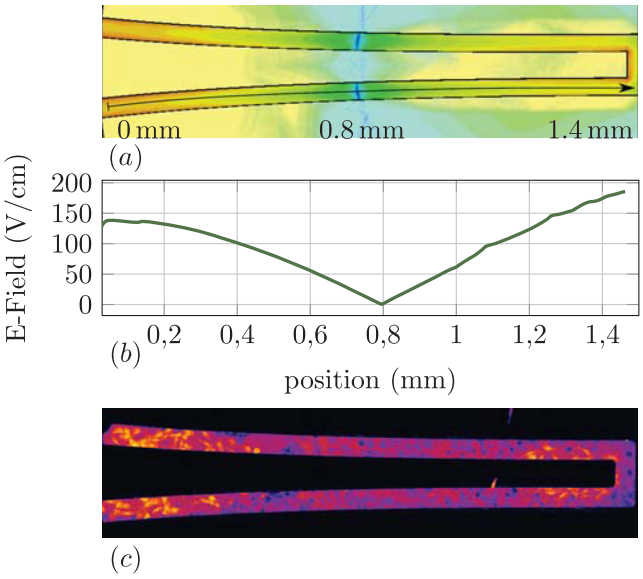

FIGURE 8. The electric field strength inside the reservoir was evaluated with full wave simulations. (a) Due to a standing wave, a local minimum occurs at the center of the reservoir. (b) The field strength was evaluated along the gap. Because the structure is symmetric, the cells are exposed to the same electric field at both sides of the transducer. (c) The cells show a location-dependent uptake which correlates to the pattern of the field strength. In contrast, the temperature is assumed to be constant due to the small dimensions.

well as the conducting silver glue (cpw to metallic frame), were considered in the model.

The dominant path for determining the temperatures and the distribution in the medium is (a). At the interface between medium and transducer the heat is transferred to the medium depending on the conductivity of the water $1/R_w$ which is well known (0.6 W/mK) and connected to the ambient temperature ϑ_a at the surface of the reservoir. There is a discrepancy between simulated and measured temperature gradients of the medium in the reservoir as thermal convection is not incorporated in the model, depicted inFigure 7 (a). In fact, temperature differences in the fluid will equalize due to density differences, which influences both the effective thermal capacitance (C_w) and the conductivity ($1/R_w$). This effect can be modeled by introducing a coefficient $0 \leq \alpha \leq 1$ and therefore, increase the conductivity of the water. Parametric sweeps were performed to match the temperature measurements with the simulations for a given input power. Figure 7 (b) shows the temperature distribution inside the reservoir for $\alpha = 0.5$ which is in good agreement to the measured temperatures of the transducer, the fluid and the surface. Simplifications were made by neglecting cross heating between the paths. For example, apart from the transducer the heated fluid volume would also be a heat source for the Rexolite reservoir. Therefore, the simulated time constant cannot match the measurements.

B. ELECTRIC FIELD STRENGTH

The maximum available output power of the portable power source (*Hittite HMC-T2240*) used during the experiments is $P_0 = 24$ dBm at 18 GHz. The attenuation of the coaxial cable and the adapter respectively, results in an measured input power level of $P_1 = 20.13$ dBm. This power level was assumed for the coupled electromagnetic-thermal simulation. Figure 8 (a) and (b) depict the field distribution and the evaluation of the electric field strength along the gap. Due to standing waves, it can be seen that a local minimum occurs at 0.8 mm and the field strength increases at the beginning and towards the end of the transducer, respectively. This distance can be validated with a calculation of the quarter wavelength of the open ended waveguide in the container which leads to: $\lambda/4 = c_0/(4 \cdot f\sqrt{\varepsilon_{\text{eff}}}) = 0.85$ mm with $\varepsilon_{\text{eff}} \approx \frac{\varepsilon_s+\varepsilon_m}{2}$, where $\varepsilon_s = 4.7$ and $\varepsilon_m = 43.2$ are the relative permittivities of the substrate and the medium at 18 GHz respectively. For the medium the Debye model of water was chosen. The simulation does not incorporate the SMA connector of the applicator, the losses of the glued Rexolite container and the conducting silver glue as well as the potentially lower conductivity of the plated gold. Therefore, the plotted field strength in Figure 8 (b) can be seen as an upper bound which was not reached during the experiments. In subplot (c) it can be seen that the uptake of the cells follow the pattern of the electric field. While higher field strength at the beginning and the end of the reservoir results in uptake, at the center of the transducer no uptake can be reported. On the other hand, because of the small dimensions and convection the temperature can be assumed to be constant all over the structure. The homogeneous temperature distribution along the transducer can also be seen in Figure 7 (a) and (b). It should be emphasized, that this observation is an evidence for microwave induced electroporation.

V. CONCLUSION

We showed the uptake of Pep-5T in adherent mammalian cells (C2C12) with a novel microwave electroporation system. Our prototype allows to monitor the uptake process

kinetics with live cell confocal microscopy and is suitable to culture, manipulate and observe cells over several days. The adherent cells were stained three days after the experiment with Calcein blue AM. Our data revealed almost no cell mortality during the treatment. However, due to the small number of affected cells, quantitative studies were not possible. Simulations and measurements showed that the temperature does not exceed 34 °C directly at the location of treatment. Control tests at different temperatures up to 42 °C show no uptake. The electric field strength in the reservoir was figured out to be dependent on the position but lower than 150 V/cm. The positive uptake correlates with the pattern of the field strength, while it was shown that the temperature is homogeneously distributed. It cannot be ruled out that a certain temperature range affects the efficiency of the process, but it should be emphasized, that microwaves are the inducing factor rather than temperature.

ACKNOWLEDGMENT

The authors acknowledge support by the German Research Foundation and the Open Access Publishing Fund of Technische Universität Darmstadt. The authors would like to acknowledge the Computer Simulation Technology AG for providing CST Studio Suite.

REFERENCES

[1] E. Neumann, M. Schaefer-Ridder, Y. Wang, and P. H. Hofschneider, "Gene transfer into mouse lyoma cells by electroporation in high electric fields," *EMBO J.*, vol. 1, no. 7, pp. 841–845, Jul. 1982.
[2] T. Kotnik, W. Frey, M. Sack, S. H. Meglič, M. Peterka, and D. Miklavčič, "Electroporation-based applications in biotechnology," *Trends Biotechnol.*, vol. 33, no. 8, pp. 480–488, Aug. 2015.
[3] D. Miklavčič, *Handbook of Electroporation*, D. Miklavčič, Ed. Tokyo, Japan: Springer, 2017.
[4] H. Li, X. Ma, X. Du, X. Cheng, and J. C. M. Hwang, "High-frequency continuous-wave electroporation of jurkat human lymphoma cells," in *IEEE MTT-S Int. Microw. Symp. Dig. (IMS)*, May 2016, pp. 1–4.
[5] Y. Zhan, Z. Cao, N. Bao, J. Li, J. Wang, T. Geng, H. Lin, and C. Lu, "Low-frequency ac electroporation shows strong frequency dependence and yields comparable transfection results to dc electroporation," *J. Controlled Release*, vol. 160, no. 3, pp. 570–576, Jun. 2012.
[6] T. Geng, Y. Zhan, and C. Lu, "Gene delivery by microfluidic flow-through electroporation based on constant DC and AC field," in *Proc. Annu. Int. Conf. IEEE Eng. Med. Biol. Soc.*, Aug./Sep. 2012, pp. 2579–2582.
[7] V. Novickij, J. Dermol, A. Grainys, M. Kranjc, and D. Miklavčič, "Membrane permeabilization of mammalian cells using bursts of high magnetic field pulses," *PeerJ*, vol. 5, p. e3267, Apr. 2017.
[8] S. Kranjc, M. Kranjc, J. Scancar, J. Jelenc, G. Sersa, and D. Miklavcic, "Electrochemotherapy by pulsed electromagnetic field treatment (PEMF) in mouse melanoma B16F10 *in vivo*," *Radiol. Oncol.*, vol. 50, no. 1, pp. 39–48, Mar. 2016.
[9] V. Novickij, I. Girkontaitė, A. Zinkevičienė, J. Švedienė, E. Lastauskienė, A. Paškevičius, S. Markovskaja, and J. Novickij, "Reversible permeabilization of cancer cells by high sub-microsecond magnetic field," *IEEE Trans. Magn.*, vol. 53, no. 11, Nov. 2017, Art. no. 2001904.
[10] W. Krassowska and P. D. Filev, "Modeling electroporation in a single cell," *Biophys. J.*, vol. 92, no. 2, pp. 404–417, Jan. 2007.
[11] H. Akiyama and R. Heller, *Bioelectrics*. Tokyo, Japan: Springer, 2017.
[12] J. Teissie, M. Golzio, and M. P. Rols, "Mechanisms of cell membrane electropermeabilization: A minireview of our present (lack of ?) Knowledge," *Biochim. Et Biophys. Acta*, vol. 1724, no. 3, pp. 270–280, Aug. 2005.
[13] T. B. Napotnik, M. Reberšek, P. T. Vernier, B. Mali, and D. Miklavčič, "Effects of high voltage nanosecond electric pulses on eukaryotic cells (*in vitro*): A systematic review," *Bioelectrochemistry*, vol. 110, pp. 1–12, Aug. 2016.
[14] T. H. P. Nguyen, Y. Shamis, R. J. Croft, A. Wood, R. L. McIntosh, R. J. Crawford, and E. P. Ivanova, "18 GHZ electromagnetic field induces permeability of Gram-positive cocci," *Sci. Rep.*, vol. 5, no. 1, p. 10980, Jun. 2015.
[15] T. H. P. Nguyen, V. T. H. Pham, V. Baulin, R. J. Croft, R. J. Crawford, and E. P. Ivanova, "The effect of a high frequency electromagnetic field in the microwave range on red blood cells," *Sci. Rep.*, vol. 7, p. 10798, Dec. 2017.
[16] Y. Shamis, A. Taube, N. Mitik-Dineva, R. Croft, R. J. Crawford, and E. P. Ivanova, "Specific electromagnetic effects of microwave radiation on escherichia coli," *Appl. Environ. Microbiol.*, vol. 77, no. 9, pp. 3017–3022, 2011.
[17] U. Kaatze, "Complex permittivity of water as a function of frequency and temperature," *J. Chem. Eng. Data*, vol. 34, no. 4, pp. 371–374, Oct. 1989.
[18] K. Nörtemann, J. Hilland, and U. Kaatze, "Dielectric properties of aqueous NaCl solutions at microwave frequencies," *J. Phys. Chem. A*, vol. 101, no. 37, pp. 6864–6869, 1997. doi: 10.1021/jp971623a.
[19] S. Xiao, I. Semenov, R. Petrella, A. G. Pakhomov, and K. H. Schoenbach, "A subnanosecond electric pulse exposure system for biological cells," *Med. Biol. Eng. Comput.*, vol. 55, no. 7, pp. 1063–1072, May 2016.
[20] S. Schmidt, M. Schüßler, Z. Luo, R. Jakoby, H. D. Herce, and M. C. Cardoso, "Compact dualmode microwave electroporation and dielectrometry tool," in *1st IEEE MTT-S Int. Microw. Symp. Dig. (IMBIOC)*, May 2017, pp. 1–3.
[21] A. Bulysheva, J. Hornef, C. Edelblute, C. Jiang, K. Schoenbach, C. Lundberg, M. A. Malik, and R. Heller, "Coalesced thermal and electrotransfer mediated delivery of plasmid DNA to the skin," *Bioelectrochemistry*, vol. 125, pp. 127–133, Feb. 2019.

SÖNKE SCHMIDT (S'16) was born in Wiesbaden, Germany, in 1987. He received the M.Sc. degree in electrical engineering from the Technische Universität Darmstadt, Germany, in 2015, where he is currently pursuing the Ph.D. degree with the Institute of Microwave Engineering and Photonics. His research interests include microwave biosensors and dielectric spectroscopy.

MARTIN SCHÜßLER received the Dipl.Ing. and Ph.D. degrees from Technische Universität Darmstadt, Darmstadt, Germany, in 1992 and 1998, respectively. He was involved in III–V semiconductor technology, microwave sensors for industrial applications, RFID, and small antennas. Since 1998, he has been a Staff Member with the Institute of Microwave Engineering and Photonics, Technische Universität Darmstadt. His current research interest includes the application of metamaterials for industrial and biomedical sensing.

CAROLIN HESSINGER received the B.Sc. degree in communication technology and the M.Sc. degree in microwave engineering from the Technische Universität Darmstadt, Darmstadt, Germany, in 2012 and 2015, respectively, where she is currently pursuing the Ph.D. degree with the Institute of Microwave Engineering and Photonics. Her current research interests include microwave sensors for medical applications, microwave ablation, and dielectric properties of tissue in the microwave region.

CHRISTIAN SCHUSTER (S'16) was born in Wiesbaden, Germany, in 1988. He received the B.Sc. and M.Sc. degrees from the Technische Universität Darmstadt, Darmstadt, Germany, in 2012 and 2015, respectively, where he is currently pursuing the Ph.D. degree with the Microwave Engineering Group, in 2015. His current research interests include tunable microwave filters and reconfigurable RF transceiver systems.

BIANCA BERTULAT was born in Dieburg, Germany. She graduated in biology from the Technische Universität Darmstadt, Darmstadt, Germany, in 2002. She received the Ph.D. degree from the Technische Universität Darmstadt, after working in Heidelberg and Darmstadt, with a focus on molecular and developmental cell biology. In 2009, she joined the Epigenetics and Cell Biology Group of Cristina Cardoso in Darmstadt and contributed to multiple interdisciplinary projects, focusing on microscopy and stem cell differentiation. Since 2018, she has been with the Department of Biochemistry, Chemistry and Pharmacy, Johann Wolfgang Goethe University Frankfurt, Frankfurt, Germany.

MARINA KITHIL received the M.Sc. degree in technical biology and the Ph.D. degree from the Technische Universität Darmstadt, Germany, in 2015 and 2018, respectively. Working in the Membrane Biophysics Working Group, her studies focused on protein sorting pathways with the main emphasis on the influence of codon usage using small viral potassium channels as a model system. Most recently, she joined the Epigenetics and Cell Biology Group of Cristina Cardoso in Darmstadt to co-develop the "microwaveporator."

M. CRISTINA CARDOSO studied biology at the University of Lisbon, Portugal. She received the Ph.D. degree in molecular biology from the New University of Lisbon, Portugal. She trained as a Postdoctoral Fellow at the Harvard Medical School, Boston, MA, USA, working on reversal of terminal differentiation of mammalian cells. She then became a Group Leader at the Max Delbrück Center for Molecular Medicine, Berlin, Germany. Since 2008, she has been a Full Professor of cell biology and epigenetics with the Department of Biology, Technische Universität Darmstadt, Germany. Her main research interest includes the cell biology of the mammalian (epi)genome during cellular proliferation and reprogramming. She is also interested in developing methods for the intracellular delivery of biomolecules. She is also a member of the American and German Cell Biology Societies and the German Society for Biochemistry and Molecular Biology.

ROLF JAKOBY was born in Kinheim, Germany, in 1958. He received the Dipl.Ing. and Dr.Ing. degrees in electrical engineering from the University of Siegen, Germany, in 1985 and 1990, respectively. In 1991, he joined the Research Center of Deutsche Telekom, Darmstadt, Germany. Since 1997, he has been a Full Professor with TU Darmstadt, Germany. He is a Co-Founder of ALCAN Systems GmbH. He is the author of more than 320 publications. He holds more than 20 patents. His research interests include chipless RFID sensor tags, biomedical sensors and applicators, tunable passive microwave/millimeter wave devices, and beam-steering antennas, using primarily ferroelectric and liquid crystal technologies. He is also a member of VDE/ITG and IEEE/MTT/AP Societies. He received an award from CCI Siegen for his excellent Ph.D., in 1992, and the ITG-Prize, in 1997, for an excellent publication in the IEEE AP Transactions. His group received 23 awards and prizes for best papers and doctoral dissertations. He is also the Editor-in-Chief of FREQUENZ, DeGruyter. He was the Chairman of the EuMC, in 2007, and the GeMiC, in 2011, and the Treasurer of the EuMW, in 2013 and 2017.